A SOLUTION OF BATTERY COOLING FOR HEV TRUCK

GIẢI PHÁP LÀM MÁT PIN CHO XE TẢI HEV

Le Minh Duc*, Nguyen Van Phuc, Le Minh Hung, Le Cong Tin

The University of Danang - University of Science and Technology, Vietnam

*Corresponding author: minhducle@dut.udn.vn

(Received: March 19, 2025; Revised: May 01, 2025; Accepted: September 08, 2025)

DOI: 10.31130/ud-jst.2025.23(9A).146

Abstract – This study presents an air-cooled battery solution for the hybrid series truck, aiming to optimize thermal efficiency and extend battery life. In the series hybrid powertrain, the battery plays an important role in providing power to the electric motor to help the vehicle operate well in working modes. However, during the charging-discharging process, the battery temperature can suddenly increase, affecting the performance, service life, and safety of the entire system. This study calculates the thermal characteristics of the battery, analyzes and optimizes the forced air cooling system. Numerical simulations are performed by ANSYS Fluent to evaluate the influence of air flow velocity at 20 m/s, battery compartment ventilation structure on heat dissipation capacity. The research results show that, the forced air cooling system can maintain the battery temperature within a safe range, reduce the risk of overheating and improve operating performance.

Keywords – Hybrid Series; Battery temperature; Battery cooling; Computational Fluid Dynamics (CFD).

Tóm tắt - Nghiên cứu này trình bày giải pháp làm mát pin bằng không khí cho xe tải hybrid kiểu nối tiếp, nhằm tối ưu hóa hiệu suất nhiệt và kéo dài tuổi thọ pin. Trong hệ thống động lực hybrid series, pin đóng vai trò quan trọng trong việc cung cấp năng lượng cho động cơ điện giúp xe vận hành tốt ở các chế độ làm việc. Tuy nhiên, trong quá trình sạc-xả, nhiệt độ pin có thể tăng cao đột ngột, ảnh hưởng đến hiệu suất hoạt động, tuổi thọ và độ an toàn của cả hệ thống. Nghiên cứu này tính toán đặc tính nhiệt của pin, phân tích và tối ưu hóa hệ thống làm mát bằng không khí cưỡng bức. Mô phỏng số được thực hiện bởi ANSYS Fluent để đánh giá ảnh hưởng của tốc độ dòng khí với vận tốc 20 m/s, cấu trúc thông gió khoang chứa pin đến khả năng tản nhiệt. Kết quả nghiên cứu cho thấy, hệ thống làm mát cưỡng bức bằng không khí có thể duy trì nhiệt độ pin trong phạm vi an toàn, giảm nguy cơ quá nhiệt và nâng cao hiệu suất vận hành.

Từ khóa - Hybrid nối tiếp; Nhiệt độ pin; Làm mát pin; Mô phỏng số CFD.

1. Overview

The rapid increase in greenhouse gas concentrations over recent decades has had adverse effects on the environment and climate. This has led to the warming of the atmosphere, land, cryosphere, and oceans. Extreme weather and climate phenomena, such as heavy rainfall and frequent heatwaves occurring in most regions worldwide, are clear evidence of these impacts. According to the latest research published in Earth System Science Data, annual greenhouse gas emissions have reached a record high, equivalent to 54 billion tons of carbon dioxide (CO_2) released into the atmosphere. This has resulted in a rapid rise in Earth's surface temperature. Data from 2013 to 2022 also indicate that the average temperature increased by 0.2°C every decade, with global warming projected to reach an increase of 1.5°C by 2050 [1-2]. The rise in greenhouse gas concentrations not only negatively affects the environment but also poses significant challenges to the transportation sector – one of the largest sources of CO_2 emissions globally.

According to a report by the International Energy Agency (IEA), the transportation sector accounts for approximately 25% of total CO_2 emissions, with the majority originating from vehicles powered by fossil fuels. Notably, freight transport by truck contributes significantly to emissions due to high fuel consumption and continuous operation. Amid rising freight transport demand, transitioning to clean and high-efficiency vehicles is an important solution to mitigate environmental impact.

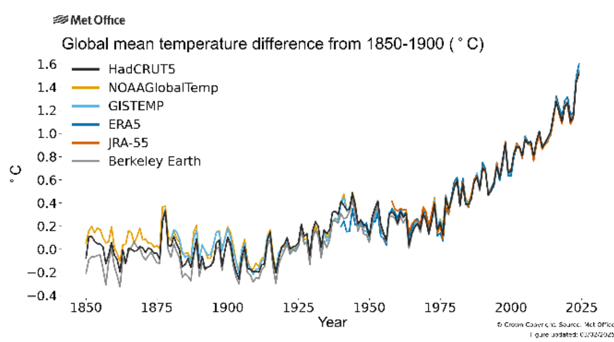

Figure 1. *Data compiled by the Met Office from regions on the difference in global average annual temperature compared to pre-industrial times [2]*

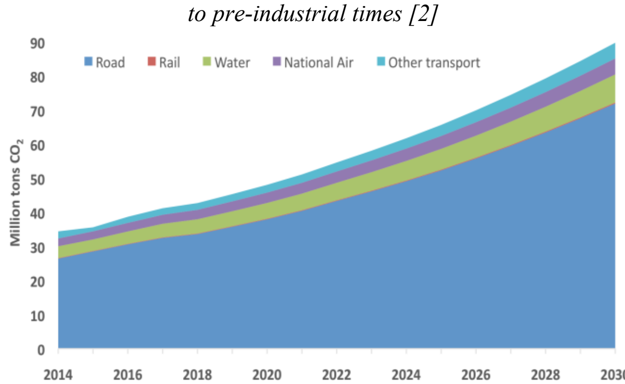

Figure 2. *Forecast of CO_2 emissions of transport sub-sectors [3]*

In Vietnam, the KIA Frontier light truck is among the most widely used models for goods transportation, manufactured and assembled by Thaco. Statistics from Thaco indicate that nearly 6,000 KIA Frontier trucks are sold annually in the Vietnamese market, accounting for nearly 30% of the light truck segment [4]. However, with conventional internal combustion engines, these KIA Frontier trucks contribute substantially to CO_2 emissions and environmental pollution. In response to emission reduction roadmaps and Vietnam's commitments, converting existing conventional vehicles to hybrid models is essential.

This paper presents a battery cooling solution for light trucks that have been converted from conventional powertrains (internal combustion engines) to hybrid powertrains. The hybrid powertrain not only offers environmental benefits but also enhances the efficiency and economic performance of trucks. The hybrid light truck is designed based on the specifications of the Kia Frontier (Thaco) [4]. For the hybrid powertrain to operate stably, the battery plays a crucial role in storing and supplying energy to the electric motor. During charging and discharging, the battery generates heat due to energy losses, causing its temperature to rise, which affects operational efficiency, lifespan, and system safety. If not effectively controlled, excessive battery temperatures can lead to capacity degradation, reduced electrochemical performance, and even overheating or fire hazards. Therefore, the battery cooling system is a critical factor in ensuring stable and sustainable battery operation within the temperature range of 15–40°C [5-6].

Various thermal management technologies for battery modules in electric vehicles (EVs) and hybrid electric vehicles (HEVs) have been developed over the past decades, including air cooling [7, 8], liquid cooling [9, 10], phase change material (PCM) cooling [11, 12], heat pipe cooling [13, 14], and other combined cooling methods [15, 16]. Among these methods, researchers have concluded that liquid cooling is widely used but incurs high costs and has low reliability [17]; PCM cooling cannot continuously dissipate heat from battery cells due to long reaction times when the material hardens [18]; heat pipe cooling is difficult to actively control temperature changes due to its passive cooling mechanism, and it also presents issues of complex structure and high energy consumption [19]. In contrast, air cooling has been extensively researched and applied due to its simple structure, low cost, high reliability, and ease of maintenance. Studies on air cooling technology have also shown that forced air cooling significantly improves the cooling performance of battery modules in EVs and HEVs [20, 21]. Therefore, in this study, forced air cooling is prioritized for hybrid truck batteries due to its simple system structure, low cost, and ease of maintenance.

2. Hybrid truck powertrain

The series hybrid powertrain is one of the common configurations of hybrid drive systems, where the internal combustion engine does not directly drive the wheels but only supplies energy to the generator, which then charges the battery and provides electricity to the electric motor for vehicle operation. This helps optimize fuel consumption, reduce greenhouse gas emissions, and enhance overall efficiency. Compared to other hybrid systems, such as parallel hybrid or series-parallel hybrid, the series hybrid is chosen for trucks due to its ability to optimize fuel consumption, reduce mechanical wear (as there is no clutch in the mechanical linkage), high flexibility in engine and generator placement, and consistent performance.

In the series hybrid system, the electric motor is the primary drive source, delivering high torque from startup, enabling smooth acceleration and stable performance when carrying heavy loads. Additionally, the internal combustion engine operates in its optimal efficiency range to charge the battery or supply electricity, significantly reducing fuel consumption compared to traditional engines. Another important benefit of the series hybrid system is reduced mechanical wear, as there is no need for a conventional transmission, lowering maintenance costs, especially crucial for trucks operating under harsh conditions.

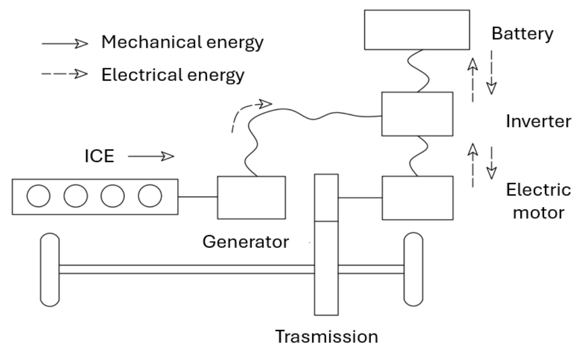

Figure 3. *HEV series hybrid vehicle powertrain diagram [7]*

The system also supports regenerative braking, which recovers energy lost during braking, improving vehicle range and reducing emissions. Moreover, with its flexible architecture, the series hybrid system can easily integrate larger battery systems or renewable energy sources, allowing the truck to operate in full electric mode (EV Mode) when necessary. This helps meet stricter future emission requirements without changing the basic structure of the drive system. Thanks to these advantages, the series hybrid system is an ideal solution for freight trucks, especially popular light trucks in Vietnam, such as the Kia Frontier, operating in urban areas or on routes requiring frequent stops and starts, thereby enhancing operational efficiency and moving towards a sustainable transportation system. Figure 3 presents the schematic of the series hybrid powertrain system for HEV trucks.

3. Battery cooling solution for HEV trucks

The battery cooling system is designed to control temperature within the safe range (15–40°C) to maintain performance and extend battery life in series hybrid vehicles (HEV). If the battery temperature exceeds the limit, its charging and discharging efficiency will decrease, its lifespan will shorten, and the risk of overheating increases. Currently, air cooling is the simplest and most common method in hybrid vehicles due to its low cost, ease of implementation, and maintenance [5-8]. This system uses fans or forced airflow to dissipate heat from the battery surface, preventing overheating without requiring complex cooling systems like liquid cooling. Compared to other methods, air cooling offers significant advantages in cost, compact design, and does not require periodic inspections as with liquid cooling systems [20, 21]. However, this method has limitations in heat dissipation capability, especially when ambient temperatures are high, so it must be optimized by using high-power fans, rational airflow design, and sensors to flexibly adjust fan speed. Thanks to these advantages, air cooling is considered the most suitable solution for hybrid trucks, ensuring stable operational performance, extending battery life, and optimizing energy consumption.

3.1. Battery cooling design

With the forced air cooling approach, the model must be designed so that the gap between individual battery cells is optimized to ensure efficient airflow, helping to evenly reduce temperature across cells without obstructing airflow. The standard gap typically ranges from 2–5 mm, optimizing heat dissipation without reducing the energy density of the battery system [23-25]. If the gap is too small (< 2 mm), airflow may be restricted, causing blockages and reducing cooling efficiency, potentially leading to temperature differences between battery cells. Conversely, if the gap is too large (> 5 mm), the battery system occupies more space, reducing energy density and possibly resulting in poor cooling due to excessive airflow dispersion. Therefore, the selection of an appropriate gap size should be based on airflow velocity and pressure, heat dissipation system structure, and cell shape to ensure effective cooling system operation (Figure 4). An axial fan with a power of approximately 60 W and a rotational speed of 20,000 rpm is selected to generate cooling airflow through the battery cells. The inlet airflow velocity is set at 20 m/s [26].

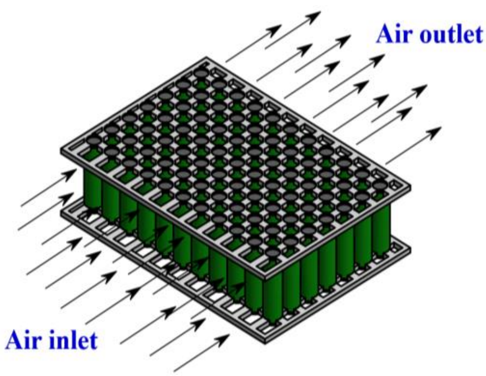

Figure 4. *Forced air battery cooling scheme on a battery module designed for the HEV truck*

Figure 4 describes the battery module model designed with a total of 77 cells per module, with cells spaced 4 mm apart to ensure optimal heat dissipation gap standards. A battery pack contains a total of 9 modules, installed with a 20 mm gap between modules. The total number of cells in the battery pack is 693. The battery pack's shape and size are designed based on actual installation conditions in the HEV truck (Figure 5). The selected cell for the model is the Lithium-ion NCR18650GA battery, widely used in electric vehicles (EVs), hybrid vehicles (HEVs), electronic devices, and energy storage. Thanks to its outstanding advantages, the battery can provide durable energy, significantly reducing voltage drop. The maximum discharge current reaches up to 10A, meeting high power demands, while its low internal resistance minimizes energy loss and maintains stable performance. The battery's long lifespan reduces replacement and maintenance costs. Panasonic's advanced safety technology ensures high reliability, reducing the risk of overheating and short circuits. The NCR18650GA lithium-ion battery does not contain toxic metals such as cadmium or mercury, making it environmentally friendly and offering a longer service life than traditional batteries.

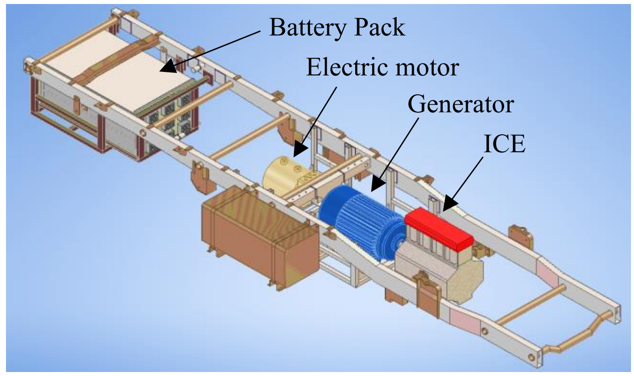

Figure 5. *Battery pack arrangement on the chassis of the HEV truck*

Table 1. *Specifications of NCR18650GA Lithium-ion Battery*

Properties	Value
Model	NCG18650GA (Panasonic)
Type	18650 Lithium-ion Rechargeable
Rated voltage	3.7 V
Charging end voltage	4.2 V
Capacity	3400~3500 mAh
Max. discharge current	Max 10 A
Average internal resistance	21~25m W
Number of charge and discharge cycles	1000 times
Weight	46 g

3.2. Numerical simulation with ANSYS Fluent

3.2.1. Input parameter setup

In this study, simulations were performed using ANSYS FLUENT 2021R1, applying CFD methods in a 3D simulation space to calculate temperature and airflow in the forced air battery cooling system. The maximum battery temperature, temperature and pressure differences among cells were determined to evaluate the cooling system's efficiency, forming a database for optimizing air cooling systems. CFD simulation methods provide highly accurate results and are widely trusted by researchers [27-31].

The standard k-ε turbulence model was selected for simulation (Table 2). Enhanced Wall Treatment improves accuracy when working with thin turbulent layers, such as flow near battery surfaces and in narrow air channels close to walls. Heat transfer phenomena-conduction, convection, and radiation-were activated (Table 3).

The inlet airflow velocity was set at 20 m/s at a temperature of 300 K. Setting airflow velocity, temperature, and material parameters during simulation is crucial to accurately reflect real-world conditions and evaluate cooling effectiveness. Airflow velocity affects heat exchange and pressure loss, while air temperature determines the temperature difference between the battery and the cooling environment.

Table 2. *Initial simulation conditions*

Model	Settings
Space	3D
Time	Unsteady, 1st-Order Implicit
Vicous	Standard k-epsilon turbulence model
Wall Treatment	Enhanced Wall Treatment
Heat Transfer	Enabled

Table 3. *Physical parameters of simulation model*

Fluid-Air	
Density	1.225 kg/m^3
Cp	1006.43 J/(kg.K)
Thermal Conductivity	0.0242 W/(m.K)
Viscosity	1.789e-05 kg/(m.s)
Molecular Weight	28.966 kg/kmol
Thermal Expansion Coefficient	0
Speed of Sound	none
Solid-Lithium	
Density	2722 kg/m^3
C_p	1200 J/(kg.K)
Thermal Conductivity	0.2 W/(m.K)

The initial temperature for the battery was set at 40°C (313 K), which is the maximum within the stable operating range for lithium batteries, to assess the effectiveness of the cooling system in temperature control. In practice, if the battery operating temperature exceeds 40°C for extended periods, necessary adjustments to the cooling system must be made.

3.2.2. Mesh parameter setup

In this study, tetrahedral cells were used for the 3D air space, and mixed cells were used for the battery pack and module models. Tetrahedral cells have four triangular faces, while mixed cells combine different cell types, optimizing mesh for complex structures and balancing accuracy and computational efficiency [32-36]. These two mesh types support flexible calculations and provide high reliability. Mesh size determination was performed to ensure convergence and minimize simulation time. The convergence results for battery temperature showed that the module model had 927,387 elements, while the pack model had 261,330 elements [37]. Specific mesh parameters for the simulation are presented in Tables 4 and 5. Mesh shapes for the battery module and pack are shown in Figures 6, 7, and 8.

Table 4. *Grid properties for a battery module*

Mesh Size			
Cells	Faces	Nodes	
927387	2700654	305909	
Mesh Quality			
Name	Type	Min Orthogonal Quality	Max Aspect Ratio
Air	Tet cell	0.21450482	16.832598
Cellwall	Mixed Cell	0.43489167	10.411489

Table 5. *Grid properties for a battery pack*

Mesh Size			
Cells	Faces	Nodes	
261330	752740	86227	
Mesh Quality			
Name	Type	Min Orthogonal Quality	Max Aspect Ratio
Air	Tet cell	0.12738712	25.47769
module	Mixed Cell	1.0	1.7671783

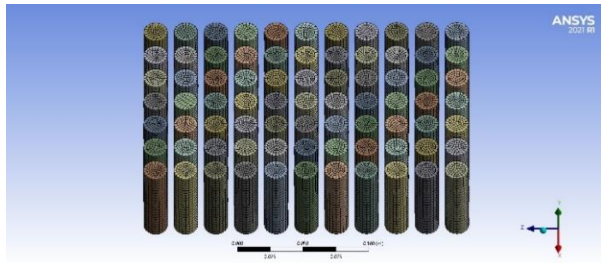

Figure 6. *Grid pattern on each battery cell*

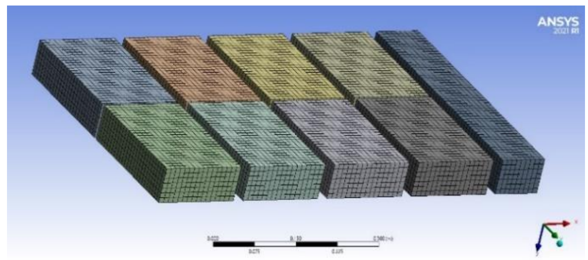

Figure 7. *Grid shape on a module*

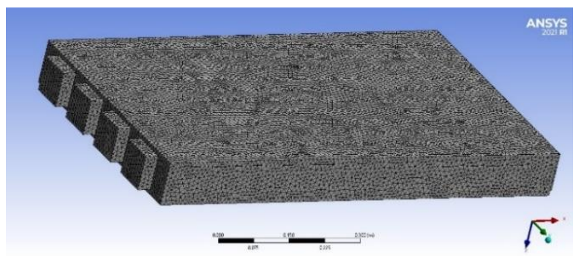

Figure 8. *Grid shape on a battery pack*

4. Results and discussion

4.1. Temperature and flow distribution in a battery module

Figures 9, 11, and 12 show the temperature variation of battery cells, outlet, and the overall module over 800 seconds of simulation. The cell temperature curve indicates that cell temperatures gradually increase over time from about 300 K to 304 K, reflecting heat accumulation in the cells. The outlet temperature shows a slight increase, indicating rapid heat dissipation. The overall temperature curve shows a steady increase throughout the simulation. The differences in temperature rise among components demonstrate the system's heat exchange and cooling capabilities, helping to assess cooling effectiveness and determine necessary adjustments to maintain pack temperature within the safe operating range.

Figures 10, 13, and 16 describe the temperature distribution of individual battery cells within the module. Cells at the rear have higher temperatures due to less airflow impact. The highest temperature reaches approximately 307 K, indicating stable cooling system performance.

Although the initial cell temperature was set at 313 K, it quickly stabilized around 307 K. Combined with the results shown in Figures 14, 15, 17, 18, 19, and 20, the pressure and velocity distribution of airflow acting on each cell can be observed. The maximum airflow velocity within the module reaches approximately 36 m/s, exceeding the initial set condition by 16 m/s. This velocity is achieved at the cell gaps where the flow cross-section narrows. The velocity field cross-sections show vortex regions formed at module corners, especially between the two fans.

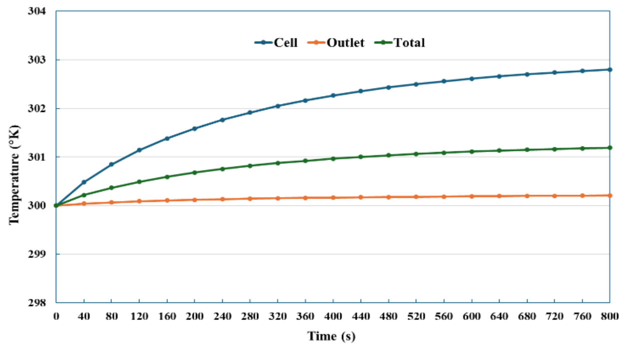

Figure 9. *Temperature variation in battery module*

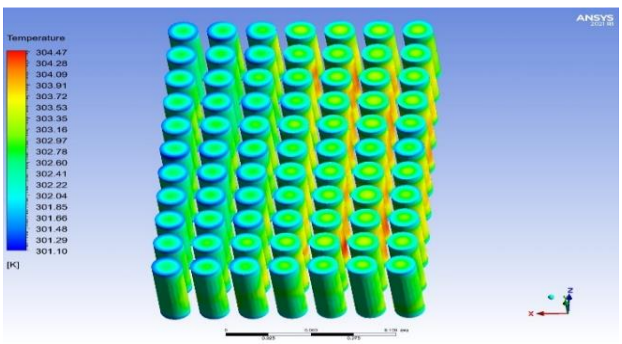

Figure 10. *Temperature distribution across each battery cell*

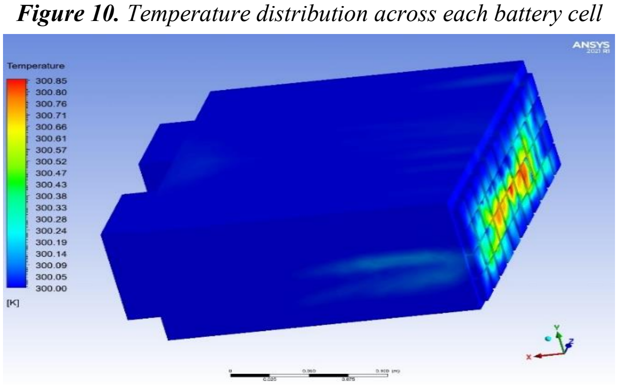

Figure 11. *Overall temperature distribution of a module*

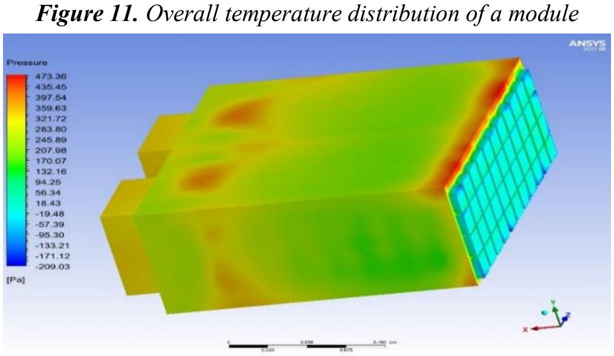

Figure 12. *Overall pressure distribution of a module*

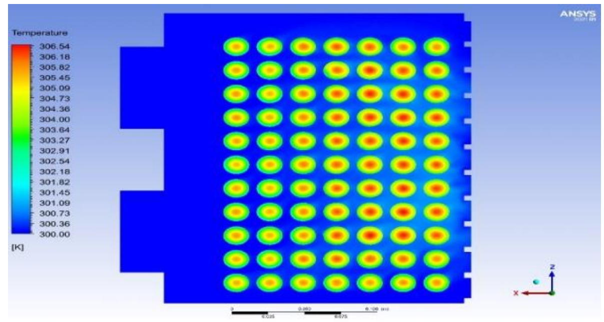

Figure 13. *Temperature distribution in a module along the cross-section*

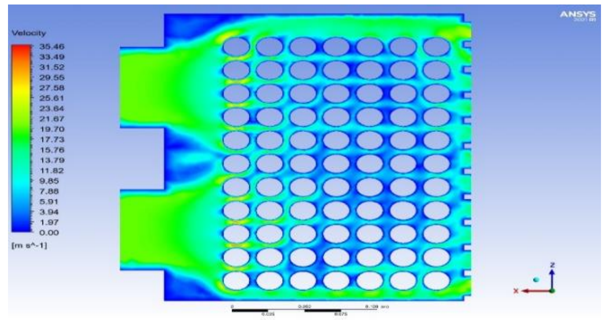

Figure 14. *Air velocity distribution in a module along the cross-section*

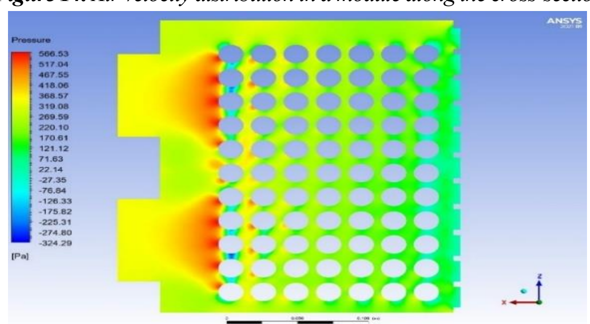

Figure 15. *Pressure distribution in a module along the cross-section*

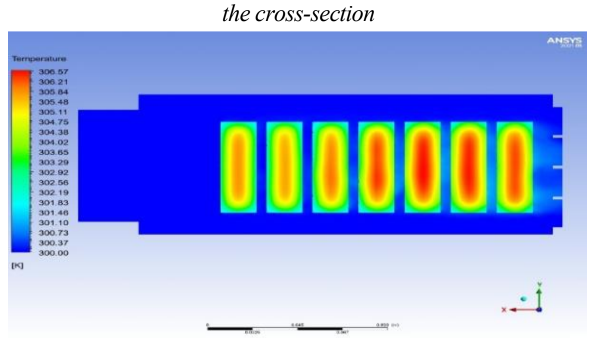

Figure 16. *Temperature distribution in a module along the longitudinal section*

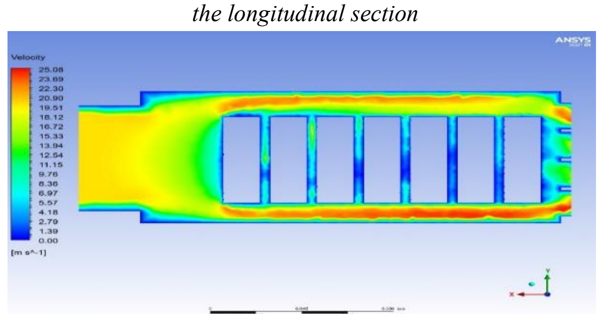

Figure 17. *Air velocity distribution in a module along the longitudinal section*

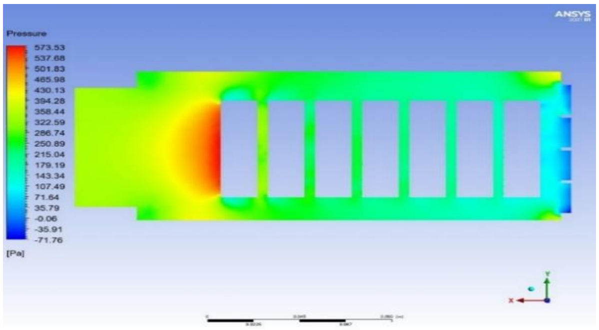

Figure 18. Pressure distribution in a module along the longitudinal section

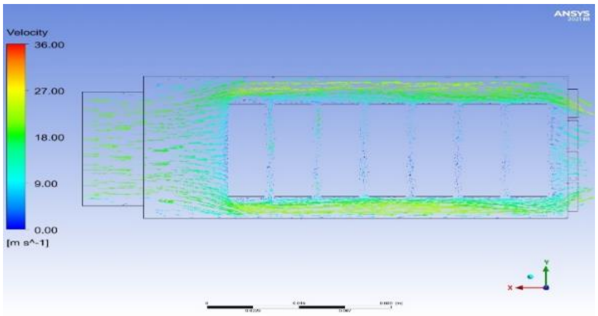

Figure 19. Velocity field distribution in a module along the longitudinal section

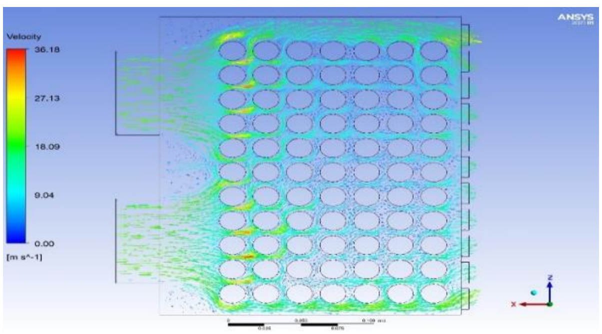

Figure 20. Velocity field distribution in a module along the cross-section

4.2. Temperature and flow distribution in a battery pack

Figure 21 shows the temperature distribution in a battery pack over time. Compared to Figure 9, the temperature of each module increases more steadily over the simulation period, peaking at approximately 308.5 K. Additionally, Figures 21, 22, and 23 show that the outlet temperature increases insignificantly, demonstrating effective heat dissipation. Although the temperature differs from the single module simulation, the outlet temperature remains similar, with no significant difference between the two simulations. For overall temperature (Total), the pack simulation results show a change of about 2°C compared to the module simulation. However, this change is negligible, as a pack contains 9 modules arranged as shown in Figure 7, totaling 693 cells. Therefore, the overall temperature increase is unavoidable. With such a temperature, the cooling design is shown to be effective.

Simulation results for a battery pack show that the external module temperature after cooling reaches only about 309 K (Figure 22). However, Figures 25 and 26 indicate that the internal temperature of each module can reach up to 310 K. This demonstrates the difference between single module and pack simulations, with cell temperature in a module simulation reaching only about 306 K. With module temperatures of about 37°C, this value is within the optimal operating range for the battery. Compared to the initial module temperature setup in the pack simulation, a reduction of about 3°C was achieved over the same simulation period. This indicates that the system still operates efficiently even if cell temperature approaches unsafe levels during charging, ensuring the battery's optimal performance and helping to minimize unwanted electrode layer formation, limiting degradation, and maintaining battery capacity.

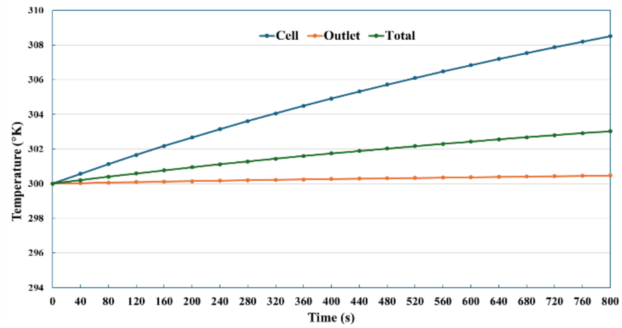

Figure 21. Temperature distriburion in a battery pack

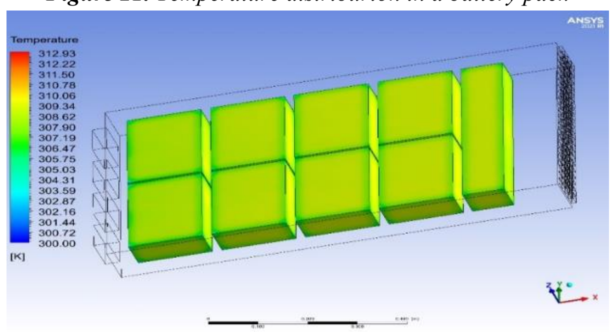

Figure 22. Temperature distribution on each battery module

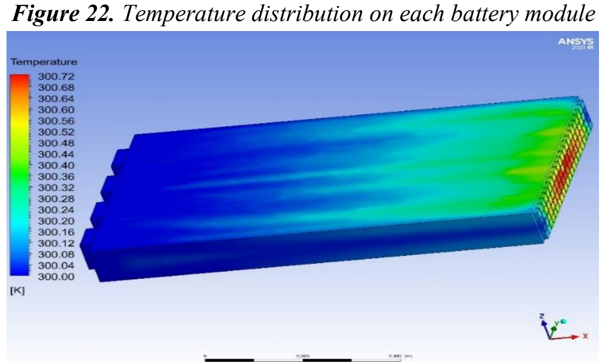

Figure 23. Overall temperature distribution of a battery pack

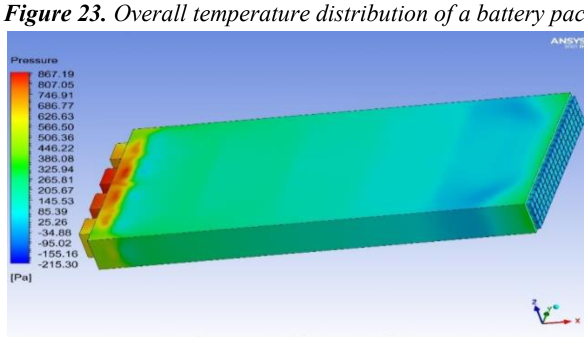

Figure 24. Overall pressure distribution of a battery pack

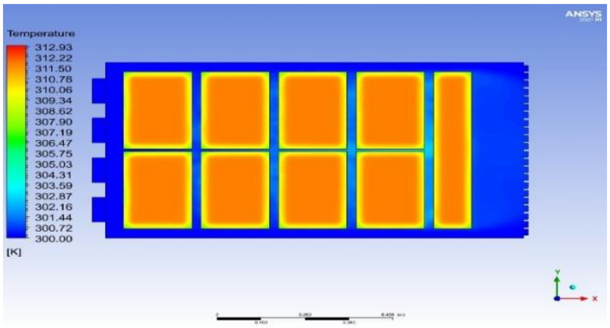

Figure 25. *Temperature distribution in a battery pack in cross-section*

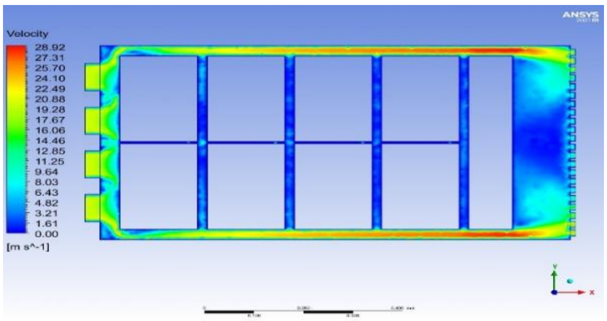

Figure 26. *Airflow velocity distribution in a battery pack in cross-section*

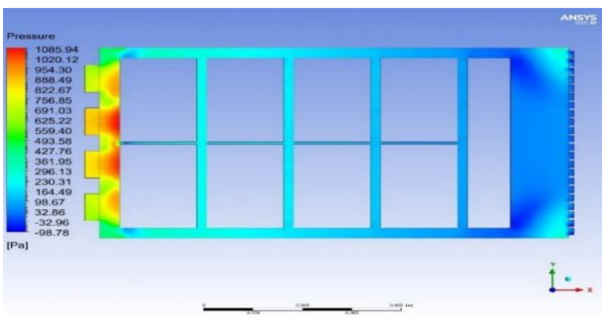

Figure 27. *Pressure distribution in a battery pack in cross-section*

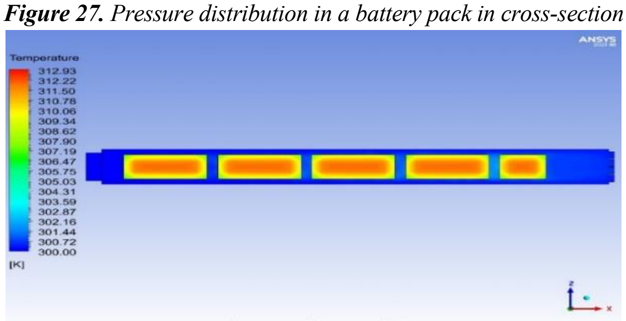

Figure 28. *Temperature distribution in a battery pack in longitudinal section*

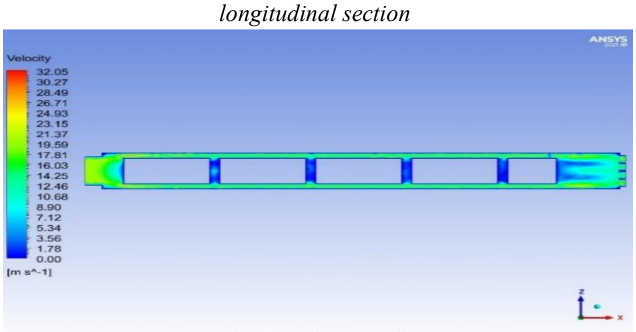

Figure 29. *Airflow velocity distribution in a battery pack in longitudinal section*

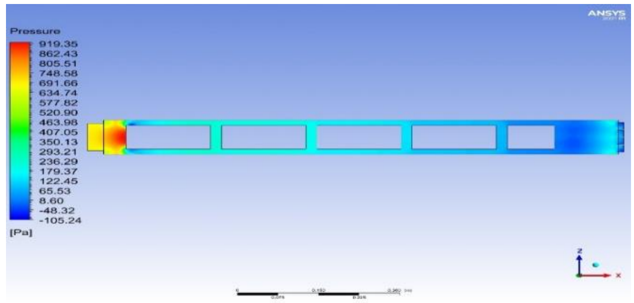

Figure 30. *Pressure distribution in a battery pack in longitudinal section*

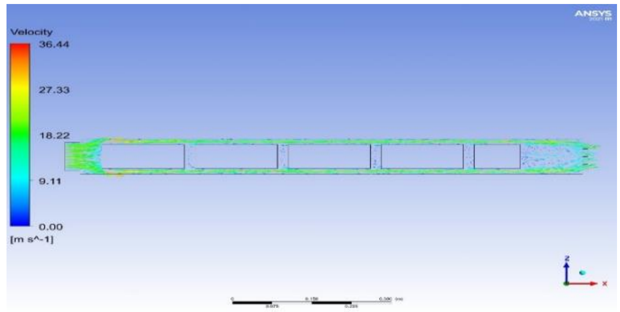

Figure 31. *Velocity field distribution in a battery pack along the longitudinal cross-section as a vector*

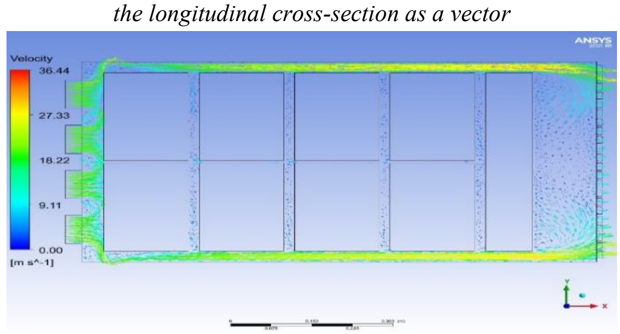

Figure 32. *Velocity field distribution in a battery pack in cross-section*

Regarding airflow velocity and pressure through the battery pack, calculations show that these quantities are still unevenly distributed, affecting cooling efficiency. Specifically, airflow tends to concentrate at the edges and inlets of the pack, where velocity is higher due to pressure buildup and flow shape changes as air enters the system. Conversely, the area between modules has lower velocity, possibly due to increased air resistance as the flow passes through narrow gaps between cells.

5. Conclusion

This study simulates and evaluates the feasibility of a battery cooling solution for HEV trucks with a series hybrid powertrain based on the Kia Frontier light truck. Using forced air cooling, the optimal gap between battery cells was selected as 4 mm. The airflow velocity was set at 20 m/s, provided by a cooling fan with a power of approximately 60 W and a rotational speed of 20,000 rpm. The initial temperature for the battery cells to evaluate cooling effectiveness was set at 40°C (313 K). Simulation results for both a battery and a pack show that battery temperature control is maintained stably within the safe operating range, helping to minimize capacity degradation and thermal imbalance in the battery pack. The results confirm the suitability of the proposed battery cooling solution for HEV trucks, but experimental validation and further refinements are needed to ensure optimal airflow, better cell contact, lower pressure loss, and reduced turbulence for improved heat exchange.

Acknowledgments: This research is funded by the Ministry of Education and Training through the project code B2024.DNA.14.

REFERENCES

[1] L.M. Khai, "Decision 687/QD-TTg 2022 approving the Scheme on development of circular economy in Vietnam", *vanban.chinhphu.vn*, June 7, 2022. [Online]. Available: https://vanban.chinhphu.vn/?pageid=27160&docid=205921, [Accessed March 16, 2025].

[2] World Meteorological Organization (WMO), "State of the Global Climate 2020", World Meteorological Organization, Geneva 2, Switzerland, WMO report 1264, June 2020.

[3] J. E. Oh, M. Cordeiro, J. A. Rogers, K. Nguyen, D. Bongardt, L. T. Dang, and V. A. Tuan, "Addressing climate change in transport: Volume 1: pathway to low-carbon transport" *Vietnam Transport Knowledge Series*, 2019.

[4] THACO, "KIA FRONTIER", *thacoauto.vn*, March 09, 2024. [Online]. Available: https://www.thacoauto.vn/en/thuong-hieu/kia-frontier, [Accessed March 16, 2025].

[5] Ma, Shuai, et al., "Temperature effect and thermal impact in lithium-ion batteries: A review*", Progress in Natural Science: Materials International,* vol. 28, no. 6, pp. 653-666, 2018.

[6] A. Sharm, M. Khatamifar, W. Lin, and R. Pitchumani, "A state-of-the-art review on numerical investigations of liquid-cooled battery thermal management systems for lithium-ion batteries of electric vehicles", *Journal of Energy Storag*e, vol. 101, pp. 113844, 2024. https://doi.org/10.1016/j.est.2024.113844

[7] K. Chen, M.X. Song, W. Wei, and S.F. Wang, "Structure optimization of parallel aircooled battery thermal management system with U-type flow for cooling effciency improvement", *Energy*, vol. 145 pp. 603–613, 2018. https://doi.org/10.1016/j.energy.2017.12.110

[8] Z. Lu, X.L. Yu, L.C. Wei, Y.L. Qiu, L.Y. Zhang, X.Z. Meng, and L.W. Jin, "Parametric study of forced air cooling strategy for lithium-ion battery pack with staggered arrangement", *Appl. Therm. Eng.*, vol. 136, pp. 28–40, 2018. https://doi.org/10.1016/j.applthermaleng.2018.02.080

[9] C.R. Zhao, W.J. Cao, T. Dong, and F.M. Jiang, "Thermal behavior study of discharging/ charging cylindrical lithium-ion battery module cooled by channeled liquid flow", *Int. J. Heat Mass Transf.*, vol. 120, pp. 751–762, 2018. https://doi.org/10.1016/j.ijheatmasstransfer.2017.12.083

[10] T.S. Zhang, Q. Gao, G.H. Wang, Y.L. Gu, Y. Wang, W.D. Bao, and D.Z. Zhang, "Investigation on the promotion of temperature uniformity for the designed battery pack with liquid flow in cooling process", *Appl. Therm. Eng.*, vol. 116, pp. 655–662, 2017.

[11] L. Lanniciello, P.H. Biwole, and P. Achard, "Electric vehicles batteries thermal management systems employing phase change materials", *J. Power Sources*, vol. 378, pp. 383–403, 2018.

[12] Y.Q. Xie et al., "Experimental and numerical investigation on integrated thermal management for lithium-ion battery pack with composite phase change materials", *Energy Convers. Manag.*, vol. 154, pp. 562–575, 2017. https://doi.org/10.1016/j.enconman.2017.11.046

[13] J.L. Liang, Y.H. Gan, and Y. Li, "Investigation on the thermal performance of a battery thermal management system using heat pipe under different ambient temperatures", *Energy Convers. Manag.*, vol. 155, pp. 1–9, 2018. https://doi.org/10.1016/j.enconman.2017.10.063

[14] L.Y. Feng *et al.,* "Experimental investigation of thermal and strain management for lithium-ion battery pack in heat pipe cooling", *J. Energy Storage*, vol. 16, pp. 84–92, 2018. https://doi.org/10.1016/j.est.2018.01.001

[15] W. X. Wu, X. Q. Yang, G. Q. Zhang, K. Chen, and S. F. Wang, "Experimental investigation on the thermal performance of heat pipe-assisted phase change material based battery thermal management system", *Energy Convers. Manag.*, vol. 138, pp. 486–492, 2017. https://doi.org/10.1016/j.enconman.2017.02.022

[16] J. Zhao, P. Lv, and Z. Rao, "Experimental study on the thermal management performance of phase change material coupled with heat pipe for cylindrical power battery pack", *Exp. Therm. Fluid Sci.*, vol. 82, pp. 182–188, 2017. https://doi.org/10.1016/j.expthermflusci.2016.11.017

[17] L. W. Jin, P.S. Lee, X. X. Kong, Y. Fan, and S. K. Chou, "Ultra-thin minichannel LCP for EV battery thermal management", *Appl. Energy*, vol. 113, no.1, pp. 1786–1794, 2014.

[18] J. Kim, J. Oh, and H. Lee, "Review on battery thermal management system for electric vehicles", *Appl. Therm. Eng.*, vol. 149, pp. 192–212, 2019. https://doi.org/10.1016/j.applthermaleng.2018.12.020

[19] T. Deng, Y. Ran, G.D. Zhang, X. Chen, and Y.Q. Tong, "Design optimization of bifurcating mini-channels cooling plate for rectangular Li-ion battery", *Int. J. Heat Mass Transf.*, vol. 139 pp. 963–973, 2019. https://doi.org/10.1016/j.ijheatmasstransfer.2019.05.082

[20] K. Chen *et al.,* "Design of parallel aircooled battery thermal management system through numerical study", *Energies*, vol. 10 pp. 1677, 2017. https://doi.org/10.3390/en10101677

[21] R. D. Jilte, R. Kumar, M. H. Ahmadi, and L. G. Chen, "Battery thermal management system employing phase change material with cell-to-cell air cooling", *Appl. Therm. Eng.*, vol. 161, pp. 114199, 2019. https://doi.org/10.1016/j.applthermaleng.2019.114199

[22] J. G. Hayes and G. A. Goodarzi, *Electric Powertrain: Energy systems, power electronics and drives for hybrid, electric and fuel cell vehicles*, 1st edition. USA: John Wiley & Sons Ltd., 2018.

[23] M. Ahmadian-Elmi and P. Zhao, "Review of thermal management strategies for cylindrical lithium-ion battery packs", *Batteries*, Vol. 10, no. 2, pp. 50, 2024. https://doi.org/10.3390/batteries10020050

[24] N. Yang, X. Zhang, G. Li, D. Hua, "Assessment of the forced air-cooling performance for cylindrical lithium-ion battery packs: A comparative analysis between aligned and staggered cell arrangements". *Applied Thermal Engineering*, vol 80, pp 55-65, 2015. https://doi.org/10.1016/j.applthermaleng.2015.01.049

[25] R. Mahamud and C. Park, "Reciprocating air flow for Li-ion battery thermal management to improve temperature uniformity", *Journal of Power Sources*, vol. 196, no. 13, pp. 5685-5696, 2011.

[26] D. Chen, J. Jiang, G. Kim, C. Yang, and A. Pesaran, "Comparison of different cooling methods for lithium ion battery cells", *Applied Thermal Engineering* vol. 94, pp. 846-854, 2016.

[27] F. Chen et al., "Air and PCM cooling for battery thermal management considering battery cycle life", *Applied Thermal Engineering*, vol. 173, pp. 115154, 2020. https://doi.org/10.1016/j.applthermaleng.2020.115154

[28] K. Yu, X. Yang, Y. Cheng, and C. Li, "Thermal analysis and two-directional air flow thermal management for lithium-ion battery pack", *Journal of Power Sources*, vol 270, pp. 193–200, 2014. https://doi.org/10.1016/j.jpowsour.2014.07.086

[29] S. C. Yong and K. D. Mo, "Prediction of thermal behaviors of an air-cooled lithium-ion battery system for hybrid electric vehicles", *J. Power Sources*, vol 270, pp. 273 -280, 2014.

[30] A. A. Pesaran, "Battery thermal models for hybrid vehicle simulations", *Journal of Power Sources*, vol 110, pp 377–382, 2002.

[31] M. Safdari, R. Ahmadi, and S. Sadeghzadeh, "Numerical investigation on PCM encapsulation shape used in the passive-active battery thermal management", *Energy*, vol. 193, pp. 116840, 2020.

[32] X. Li, F. He, and L. Ma, "Thermal management of cylindrical batteries investigated using wind tunnel testing and computational fluid dynamics simulation", *Journal of Power Sources*, vol 238, pp 395–402, 2013. https://doi.org/10.1016/j.jpowsour.2013.04.073

[33] Z. Rao, Z. Qian, Y. Kuang, and Y. Li, "Thermal performance of liquid cooling based thermal management system for cylindrical lithium-ion battery module with variable contact surface", *Applied Thermal Engineering*, vol. 123, pp 1514-1522, 2017. https://doi.org/10.1016/j.applthermaleng.2017.06.059

[34] M. Wang, S. Teng, H. Xi, and Y. Li, "Cooling performance optimization of air-cooled battery thermal management system", *Applied Thermal Engineering*, vol. 195, pp 117-242, 2021. https://doi.org/10.1016/j.applthermaleng.2021.117242

[35] F. Chen *et al.,* "Air and PCM cooling for battery thermal management considering battery cycle life", *Applied Thermal Engineering*, vol. 173, pp 115-154, 2020. https://doi.org/10.1016/j.applthermaleng.2020.115154

[36] K. Chen, W. Wu, F. Yuan, L. Chen, and S. Wang, "Cooling efficiency improvement of air-cooled battery thermal management system through designing the flow pattern", *Energy*, vol. 167, pp 781-790, 2019. https://doi.org/10.1016/j.energy.2018.11.011.

[37] R. Wang, Z. Liang, M. Souri, M. N. Esfahani, and M. Jabbari, "Numerical analysis of lithium-ion battery thermal management system using phase change material assisted by liquid cooling method", *International Journal of Heat and Mass Transfer*, vol. 183 pp. 122095, 2022. https://doi.org/10.1016/j.ijheatmasstransfer.2021.122095